

Relaxation of Pressure Anisotropy Due to Alfvén-Ion-Cyclotron Fluctuations Observed in Ion-Cyclotron-Range-of-Frequency-Heated Mirror Plasmas

M. Ichimura, M. Inutake, R. Katsumata, N. Hino, H. Hojo, K. Ishii, T. Tamano, and S. Miyoshi

Plasma Research Center, University of Tsukuba, Tsukuba, Ibaraki 305, Japan

(Received 31 August 1992)

Alfvén ion-cyclotron modes are generated over a wide range of anisotropy parameter $\beta_{\perp}(T_{\perp}/T_{\parallel})^2$ in ICRF-heated central cell plasmas of the GAMMA 10 tandem mirror. The fluctuations are observed at a small driving force in the convectively unstable region predicted theoretically in an infinite plasma. Before reaching the β limit of $\beta_{\perp} = 3.52 \times (T_{\parallel}/T_{\perp})^2$, above which the absolute instability is predicted, relaxation of pressure anisotropy is observed for the first time by use of an array of diamagnetic loops together with a Faraday cup and secondary-electron emission detectors.

PACS numbers: 52.35.Qz, 52.50.Gj, 52.55.Jd

Generation of an Alfvén ion-cyclotron (AIC) instability is expected in a magnetized plasma with strong pressure anisotropy. However, there have been limited experimental works, especially in laboratory plasmas. The first experimental evidence of the AIC mode was performed in the end cell of the TMX tandem mirror [1,2]. A high β_{\perp} (the ratio of the perpendicular plasma pressure to the magnetic field pressure) plasma with strong pressure anisotropy is produced by intense neutral-beam injection (NBI) in the direction perpendicular to the magnetic field line at the midplane of the minimum- B mirror field. The AIC mode was also observed in an ion-cyclotron-range-of-frequency- (ICRF-) heated plasma in the central cell of the TARA tandem mirror [3]. The interaction between alpha particles and the generated Alfvén modes is going to be a critical subject for future fusion devices. Effects of the AIC mode on the plasma parameters were described precisely in computer simulations [4–7]. Also, rapid pitch angle scattering due to the AIC mode has been simulated in a space plasma [8]. Relaxation of the pressure anisotropy is predicted theoretically; however, a direct observation of the relaxation due to the generation of the AIC mode has not been reported in laboratory plasmas.

In this Letter we report a parametric study of the AIC fluctuation for a wide range of the anisotropy parameter, in order to compare with an available theory. We report the first observations of the anisotropy relaxation associated with the AIC mode in the ICRF-heated central cell plasma of the GAMMA 10 tandem mirror.

GAMMA 10 is a minimum- B anchored tandem mirror with axisymmetric plug/thermal-barrier regions at both ends [9,10]. The central cell is 5.6 m long with a field strength of 0.4 T at midplane. The mirror ratio is 5. The diameter of the limiter which is set near the midplane of the central cell is 0.36 m. Double half-turn antennas are located near the end of the central cell for ion heating at the fundamental ion-cyclotron resonance layer near the midplane. So-called Nagoya type-III antennas [11] are installed on the outer side of the double half-turn antennas. They are used for producing and sustaining a plas-

ma, together with hydrogen gas puffing into the central cell and short-pulse (1 ms) plasma guns at both ends [12]. In the present experiment, no other heating systems such as electron-cyclotron heating (ECH) and NBI are used. The ICRF power coupled to the plasma is 100–200 kW. Magnetic probes are set in the peripheral region near the midplane for measuring magnetic fluctuations. Since insertion of magnetic probes into the plasma core disturbs the plasma, measurements of the fluctuation have been performed only near the periphery. For estimating the anisotropy A defined as T_{\perp}/T_{\parallel} , three diamagnetic loops are set at three different z positions with different magnetic field strengths. Assuming MHD equilibrium, we can estimate the perpendicular and the parallel pressure distribution along the magnetic field line from the measured diamagnetic signal [13]. Moreover, a pitch angle distribution of ions at the midplane is measured by using a small Faraday cup [14] and secondary-electron emission detectors (SED). The axial profile of the magnetic field strength at the central cell and the locations of antennas and diagnostics are shown in Fig. 1.

When the heating rf pulse (6.2 MHz) is applied, strong ion heating and the resultant pressure anisotropy are observed under the condition that the ion-cyclotron reso-

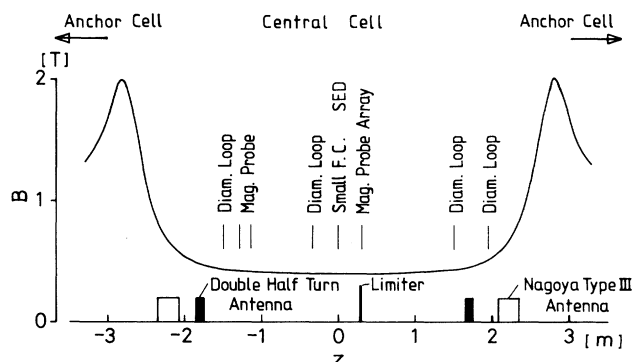


FIG. 1. Profile of the magnetic field strength of the central cell and the locations of antennas and diagnostics.

nance layer exists near the midplane of the central cell. For central values of the anisotropy A and the beta value β_{\perp} , a mode with frequencies below the ion-cyclotron frequency at the midplane is generated. Figure 2 shows the frequency spectrum measured by the magnetic probe at the location where the magnetic field strength is 1.03 times that of the midplane. Below 3 MHz, no peaks are observed. The peak at the frequency of 6.2 MHz is the applied frequency for the heating of the central cell plasma. The peak at the frequency of 9.6 MHz is also the applied frequency for the plasma production and sustainment. The cyclotron resonance layers for the frequency of 9.6 MHz exist both at the end of the central cell and near the midplane of the anchor cell. Heating of the central cell plasma by the frequency of 9.6 MHz is ineffective [15]. Peaks observed below 6.2 MHz are modes generated spontaneously in the plasma. The appearance of these fluctuations strongly depends on the pressure anisotropy A and β_{\perp} , both of which are varied by changing the heating power, the magnetic field strength and frequency, and the gas fueling rate. Figure 3(a) shows experimental data plotted in the β_{\perp} - A^2 space. Solid and open circles in the figure represent the experimental points with and without fluctuations, respectively. The value β_{\perp} is defined as $n(0)T_{\perp}$, where $n(0)$ is the density on the axis. The averaged temperature T_{\perp} is calculated from the diamagnetic signal and measured density profile under the assumption of radially uniform temperature. The symmetry of the perpendicular pressure profile with respect to the midplane is confirmed by using another diamagnetic loop located at the symmetric position. The solid curves drawn in the figure indicate maximum growth rates, $(\text{Im}\omega)_{\text{max}}/\omega_{ci}$, of 10^{-5} and 10^{-2} . These curves are calculated by using the distribution A of Ref. [16] which presents the bi-Maxwellian distribution. The boundary of the mode excitation is near the line of growth rate of 10^{-5} . Beta values for these solid circles are quite low as compared with the β_{\perp} value for the absolute instability, $\beta_{\perp} = 3.52 \times (T_{\parallel}/T_{\perp})^2$, predicted by the same theory [16]. The dashed line in the figure indicates the convective-absolute boundary. The experimental data show that AIC modes are observed also in the convective-

ly unstable region predicted by the theory. The growth time of the mode in the convectively unstable region is shorter than its existing time in the central cell. When the axial inhomogeneity effect is taken into account, stabilization of the AIC mode is predicted theoretically [17,18]. The onset condition for the absolute instability may require even larger T_{\perp}/T_{\parallel} and β than that in the uniform plasma. The experimental results indicate a discrepancy with the theory of convective-absolute boundary in axially uniform plasmas. Figure 3(b) shows the amplitudes of the fluctuation plotted as a function of the AIC drive term of $\beta_{\perp}A^2$. The amplitude increases with the AIC drive term, which is consistent with the prediction of the linear wave theory. When ICRF power increases, the AIC drive term also increases. There is no nonlinear amplitude threshold in the present experimental range.

When the magnetic field strength is changed under the condition of fixed heating frequency, the frequency of the excited modes also changes. The frequency of the excited modes is always below the ion-cyclotron frequency at the midplane of the central cell. This magnetic field dependence is consistent with the dependence deduced from the dispersion of the AIC mode. Phase differences of the excited mode are measured by magnetic probes which are distributed azimuthally on the limiter located in the mid-

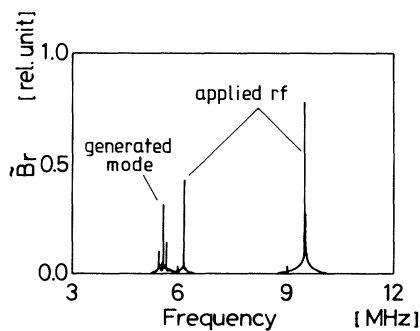


FIG. 2. Frequency spectrum of the magnetic probe signal.

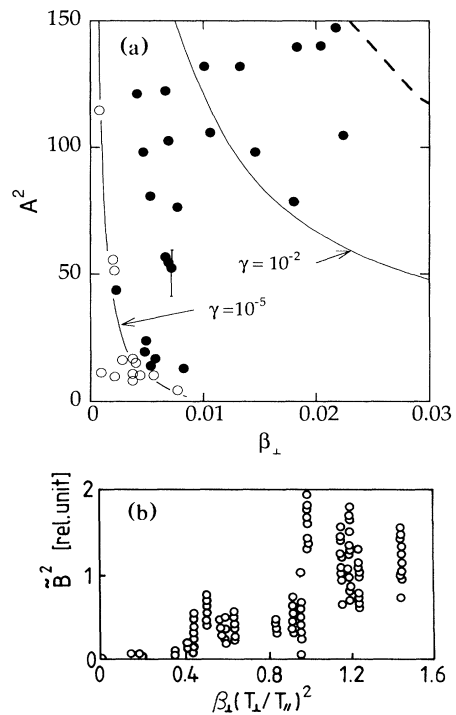


FIG. 3. (a) Experimental data on the β_{\perp} - A^2 space: (●) with fluctuations and (○) without fluctuations; solid curves indicate maximum growth rates, $\gamma = (\text{Im}\omega)_{\text{max}}/\omega_{ci}$, of 10^{-5} and 10^{-2} ; dashed line indicates the absolute boundary predicted theoretically. (b) Amplitude of the fluctuation vs $\beta_{\perp}A^2$.

plane. It is confirmed that the azimuthal mode number is $m = -1$ with a very small component of higher modes. The electromagnetic mode propagates in the direction of the ion diamagnetic drift. The polarization of the mode is measured at the mirror throat where the disturbance due to the insertion of the probe into the core region is small because of relatively cold plasma in the throat region. A left-hand polarization is confirmed in the core region. The amplitude strongly depends on the AIC drive term of $\beta_{\perp} A^2$ as shown in Fig. 3(b). These results agree well with the predictions from the dispersion relation for the AIC mode. From these characteristics of the fluctuation mentioned above, we conclude that the observed fluctuation is the AIC mode generated by the pressure anisotropy.

No electrostatic mode (loss cone mode) above the ion-cyclotron frequency is observed in the central cell. In GAMMA 10, plasmas are sustained only when the resonance layer exists near the midplane of the anchor cell neighboring both sides of the central cell [10,13]. The density in the anchor cell is nearly equal to or higher than that in the central cell. Therefore, the loss cone of the central cell is likely filled by plasmas flowing from the anchor cell.

Figure 4 shows the time evolutions of the observed sig-

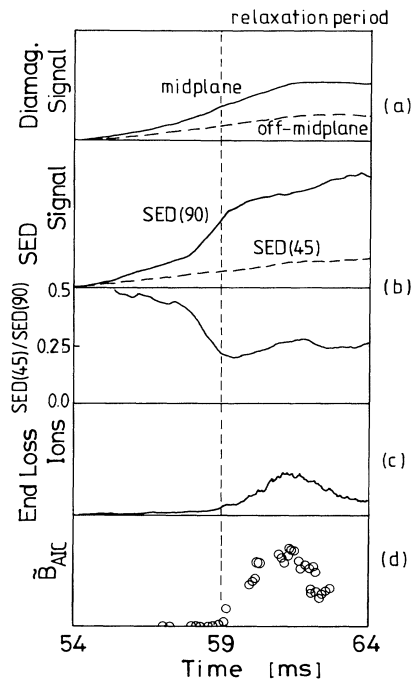


FIG. 4. Time evolutions of the experimental data: (a) diamagnetic loop signals at the midplane and off midplane; (b) signals of SED which are set at the directions of pitch angles of 90 deg, SED(90), and 45 deg, SED(45), and the signal ratio of SED(45) to SED(90); (c) end-loss ions which are near the loss cone boundary of the central cell, of which the energy is 5.1 keV; (d) amplitudes of the generated mode.

nals which indicate relaxation of the pressure anisotropy: (a) the diamagnetic loop signals at the midplane and off midplane, (b) the signals of the SEDs collecting neutral particles coming in the directions of pitch angles of 90 and 45 deg at the midplane, (c) the signal of 5.1 keV ion flux escaping from the mirror end, and (d) the amplitude of the excited mode. During this relaxation period, the density is measured by the radially scanning microwave interferometer and is almost constant around $2 \times 10^{18} \text{ m}^{-3}$. The ion temperature obtained from the midplane diamagnetic signal is above 1 keV and is increasing. Relaxation due to Coulomb collisions cannot be expected because the ion-ion collision time is of the order of 10 msec and becomes longer as the ion temperature becomes higher. The SED signal due to photons in this period is relatively small based on the measurement of the time-of-flight neutral particle analyzer which detects neutrals and photons separately [19]. The increasing rate of the signal SED(90) for charge-exchange neutrals with a pitch angle of 90 deg decreases due to the onset of the mode, while the signal SED(45) for neutrals with a pitch angle of 45 deg increases continuously. In this period the increasing rate of the diamagnetic signal near the midplane becomes slightly smaller and the diamagnetic signal off midplane maintains its increasing rate. These two phenomena suggest the relaxation of the anisotropy. The peaking during the time period before relaxation indicates the decrease of collisions. In Fig. 4(b), the ratio of the signal SED(45) to the signal SED(90) is also shown. The time evolution of the amplitude of the excited mode shown in Fig. 4(d) is obtained by using several plasma discharges. Quantitative studies of the relationship between the anisotropy relaxation and the amplitude of the AIC mode will be done in the future. Figure 4(c) is the time evolution of the end-loss ions with a pitch angle near the loss cone boundary. The end-loss ions are detected by the end-loss energy-component analyzer which measures the energy and pitch angle distributions [20]. The time evolution of the end-loss ion flux resembles that of the excited modes. The increase of the end-loss ion flux corresponds to the reduction of SED(90), which is clearly related to the onset of the AIC mode.

A small Faraday cup is used to investigate the effect of the AIC mode during the relaxation period. The small Faraday cup (FC) is inserted at the periphery of the midplane to measure the flux of ions with the same pitch angle as the angle between the magnetic field line and the FC orientation. Figure 5(a) shows the ratio of the ion flux at the end to the beginning point of the relaxation period as a function of the pitch angle. The ratio decreases toward 90 deg and becomes less than unity at 70 deg. Figure 5(b) shows the pitch angle dependence of the ion flux normalized to the ion flux with 90 deg pitch angle, where solid and open circles represent the data at the beginning point and the end of the relaxation period, respectively. The beginning point means the point at which the increasing rate of the signal begins to decrease and

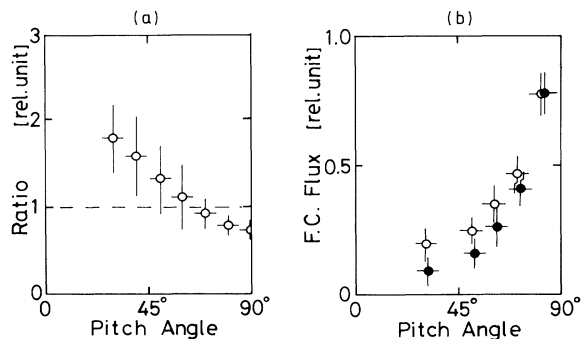


FIG. 5. (a) Ratio of the FC signal at the end to the beginning point of the period as a function of the pitch angle; (b) pitch angle distributions at the beginning point (●) and the end point (○) of the period.

the end point means the point at which the decrease stops. This confirms the relaxation of the pressure anisotropy suggested by the SED measurement. This pressure relaxation is observed well below the condition for the absolute instability.

In summary, the AIC mode is studied in an ICRF-heated mirror with a wide range of plasma parameters. Relaxation of the pressure anisotropy is directly observed for the first time in a laboratory plasma.

The authors acknowledge the GAMMA 10 group of University of Tsukuba for their collaboration. They thank Dr. Sawaya of Tohoku University for the construction of the one of the rf antennas. This work is partially supported by a Grant-in-Aid for Scientific Research from

the Ministry of Education, Science and Culture of Japan.

-
- [1] T. A. Casper and G. R. Smith, *Phys. Rev. Lett.* **48**, 1015 (1982).
 - [2] G. R. Smith, T. A. Casper, and M. J. Gerver, *Nucl. Fusion* **23**, 1381 (1983).
 - [3] S. N. Golovato *et al.*, *Phys. Fluids B* **1**, 851 (1989).
 - [4] T. Tajima, K. Mima, and J. M. Dawson, *Phys. Rev. Lett.* **39**, 201 (1977).
 - [5] T. Tajima and J. M. Dawson, *Nucl. Fusion* **20**, 1129 (1980).
 - [6] S. K. Ho *et al.*, *Phys. Fluids* **31**, 1656 (1988).
 - [7] S. K. Ho, G. R. Smith, and G. H. Miley, *Phys. Fluids B* **1**, 2040 (1989).
 - [8] M. Tanaka, C. C. Goodrich, D. Winske, and K. Papadopoulos, *J. Geophys. Res.* **88**, 3046 (1983).
 - [9] M. Inutake *et al.*, *Phys. Rev. Lett.* **55**, 939 (1985).
 - [10] S. Miyoshi *et al.*, in *Plasma Physics and Controlled Nuclear Fusion Research*, Proceedings of the Thirteenth International Conference, Washington, 1990 (IAEA, Vienna, 1991), Vol. 2, p. 539.
 - [11] T. Watari *et al.*, *Nucl. Fusion* **22**, 1359 (1982).
 - [12] M. Ichimura *et al.*, *Nucl. Fusion* **28**, 799 (1988).
 - [13] R. Katsumata *et al.*, *Jpn. J. Appl. Phys.* **31**, 2249 (1992).
 - [14] M. Ichimura *et al.*, *Jpn. J. Appl. Phys.* **30**, 854 (1991).
 - [15] M. Inutake *et al.*, *Phys. Rev. Lett.* **65**, 3397 (1990).
 - [16] G. R. Smith, *Phys. Fluids* **27**, 1499 (1984).
 - [17] T. Tajima and K. Mima, *Phys. Fluids* **23**, 577 (1980).
 - [18] G. R. Smith, W. M. Nevins, and W. M. Sharp, *Phys. Fluids* **27**, 2120 (1984).
 - [19] F. Tsuboi *et al.*, *Rev. Sci. Instrum.* **60**, 2868 (1989).
 - [20] K. Ishii *et al.*, *Rev. Sci. Instrum.* **62**, 899 (1991).